

**A Spectrum of Oxygen Isotopic Zoning Profiles in CAIs Records Varying Exposure to Distinct Protoplanetary Disk Environments.** J. I. Simon<sup>1</sup>, J. E. P. Matzel<sup>2</sup>, S. B. Simon<sup>3</sup>, P. K. Weber<sup>2</sup>, L. Grossman<sup>3</sup>, D. K. Ross<sup>4</sup>, and I. D. Hutcheon<sup>2</sup>. <sup>1</sup>NASA Johnson Space Center, Houston, TX 77058, USA (Justin.I.Simon@NASA.gov), <sup>2</sup>Lawrence Livermore National Laboratory, Livermore, CA 94551, USA, <sup>3</sup>The University of Chicago, Chicago, IL 60637, USA, <sup>4</sup>JE-23 Jacobs Technology/ESCG, P.O. Box 58477, Houston, TX 77058.

**Introduction:** In general, calcium-, aluminum-rich inclusions (CAIs) are observed to be <sup>16</sup>O-rich relative to planetary materials and are thought to record the O-isotope composition of solar nebular gas from which they grew [1]. Recent high spatial resolution O-isotope measurements afforded by ion microprobe analysis across the rims and margin of CAIs reveal systematic variations in  $\Delta^{17}\text{O}$  and suggest formation from a diversity of nebular environments [2-3]. This heterogeneity has been explained by isotopic mixing between the <sup>16</sup>O-rich solar reservoir [4] and a second <sup>16</sup>O-poor reservoir (probably nebular gas) with a “planetary-like” isotopic composition [e.g., 1, 4-5], but the mechanism and location(s) where these events occur within the protoplanetary disk remain uncertain.

The large and systematic variations in  $\Delta^{17}\text{O}$  that we found [3] within the Wark-Lovering (WL) rim and the outer margin of the interior of a compact Type A CAI, A37 from the Allende oxidized CV3 chondrite, indicate exposure of the inclusion to several distinct, nebular O reservoirs and imply the transfer of CAIs among different nebular settings within the protoplanetary disk [3]. To further investigate this hypothesis and the extent of intra-CAI O-isotope variation, a relatively unaltered compact Type A CAI, Ef-1 from the reduced CV3 chondrite Efremovka, and a Type B2 CAI, TS4 from Allende were analyzed by NanoSIMS. Our new results are equally intriguing because collectively the O-isotopic zoning patterns in the CAIs appear to reveal a progressive and systematic record of different stages of isotopic exchange with a series of distinct O-isotopic gas reservoirs.

**Samples:** Ef-1 is an ~3 x 3.5 mm convoluted compact Type A CAI composed mainly of melilite and 20-70  $\mu\text{m}$ -sized spinel locally enclosed by fassaite. It is surrounded by a ~15 to 40  $\mu\text{m}$  thick WL rim comprised from its interior outwards of spinel and pyroxene. TS4 is an ~5 x 8 mm irregularly shaped Type B2 CAI composed mainly of a partial margin of melilite ( $\text{Å}_{k35-50}$ ), 5-70  $\mu\text{m}$ -sized spinel found throughout and as palisades, fassaite, and anorthite. The latter are found towards the interior along with spinel in concentrations so high that they are in contact. TS4 is surrounded by a ~30 to 50  $\mu\text{m}$  thick WL rim comprised from its interior outwards of spinel, Ti-bearing pyroxene, Al-rich pyroxene, and an outermost band of forsterite. Secondary sodalite is found in patches at the edge of the interior. A37 is described in [3].

**Methods:** We used the NanoSIMS at LLNL to perform O-isotope measurements following the method developed by [3]. We evaluated instrumental mass fractionation (IMF) and reproducibility by analyses of terrestrial spinel, anorthite, grossular, and forsterite standards. O-isotope compositions are reported in terms of  $\delta^{17}\text{O}$  and  $\delta^{18}\text{O}$ . These values reflect the per mil difference from the reference ratios of standard mean ocean water (SMOW) such that  $\delta^i\text{O} = 10^3((^i\text{O}/^{16}\text{O})/(^i\text{O}/^{16}\text{O})_{\text{SMOW}} - 1)$  where  $i$  is either 17 or 18. Based on the range of standard analyses, the external precision was <4.0‰ (sd) for both ratios.  $\Delta^{17}\text{O}$ , defined as  $\Delta^{17}\text{O} = \delta^{17}\text{O} - 0.52 \times \delta^{18}\text{O}$ , represents the departure from the terrestrial mass fractionation (TMF) line that defines the terrestrial O reservoir. Our precision on  $\Delta^{17}\text{O}$  ranged from 1.9‰ (sd) for olivine to 3.5‰ (sd) for garnet and the difference in  $\Delta^{17}\text{O}$  among the terrestrial minerals was <2.5‰ (sd), about equal to, or less than our typical uncertainty (~3.0‰). X-ray and backscattered electron maps were obtained at NASA-JSC, UChicago, and/or LLNL before and after NanoSIMS analysis to guide ion probe traverses and to verify the mineralogy of the analysis spots.

**Results:** On O three-isotope plots, data for Ef-1 and TS4 exhibit scatter about and along the carbonaceous chondrite anhydrous mineral (CCAM) line (Figs. 1 & 2). Data for each inclusion come from ~2  $\mu\text{m}$  spot analyses along traverses spanning across their WL rims and coarse-grained interiors (Fig. 3a,b,c). Like A37, data from both Ef-1 and TS4 exhibit heterogeneous <sup>16</sup>O abundances (>20‰). Yet, compared to A37, the interior melilites in Ef-1 and TS4 are more homogeneous and <sup>16</sup>O-poor. Exceptions include small but systematic  $\Delta^{17}\text{O}$  decreases (~5‰) at the outermost edge of Ef-1 (Fig. 3a) and possibly within the interior of TS4 (Fig. 3b). Spinel from interiors of all studied CAIs are <sup>16</sup>O-rich ( $\Delta^{17}\text{O} \leq -20\text{‰}$ ). The O-isotopic composition of fassaite in TS4 is similar to spinel, and that of anorthite in TS4 is similar to its melilite. Sodalite in the margin of TS4 has planetary-like, <sup>16</sup>O-poor compositions.

WL rims on Ef-1 and TS4 are thinner than on A37. Yet, a similar isotopic stratigraphy exists within rims of all three CAIs: (1) spinel is <sup>16</sup>O-rich ( $\Delta^{17}\text{O} \leq -15\text{‰}$ ); (2) pyroxene becomes relatively <sup>16</sup>O-poor towards the interior; and (3) olivine, where present, is variable.

**Discussion:** The mineral textures and compositions of the studied CAIs indicate crystallization from a melt (e.g., [6-7]). At issue, are the differences found be-

tween the O-isotope zoning profiles among the studied CAIs (Fig. 3a,b,c). The O-isotopic zoning of A37, which cannot be explained by igneous processes and is likely secondary in origin [3] is useful to consider when investigating CAIs like Ef-1 and TS4 that exhibit distinct mineral specific O-isotopic zoning profiles. The O-isotopic compositions of spinel from the interiors of Ef-1 and TS4 are similar to the <sup>16</sup>O-rich melilites in the interior of A37. The difference between the <sup>16</sup>O-poor compositions ( $\Delta^{17}\text{O}\sim 0\text{‰}$ ) of melilites in the interiors of Ef-1 and TS4 and their spinel ( $\pm$ fassaite) ( $\Delta^{17}\text{O}\sim 20$  to  $-25\text{‰}$ ) likely reflects their differing amounts of O-isotopic exchange with <sup>16</sup>O-poor nebular gas. Additionally, the new data on spinel ( $\Delta^{17}\text{O}=-30\text{‰}$ ) from A37 that match the solar value of [4] imply that the <sup>16</sup>O-rich interior spinel data from Ef-1 and TS4 and the <sup>16</sup>O-rich melilite of A37 also reflect some exchange with a <sup>16</sup>O-poor reservoir.

Comparing the degree of <sup>16</sup>O depletion of the studied CAIs reveals a progressive trend (Ef-1>TS4>A37) of exchange that is decoupled from their mineralogical evidence of alteration. The possibility that spinel in the interiors of Ef-1 and TS4 has undergone some isotopic exchange (as seen by their relative depletion in <sup>16</sup>O and the  $\Delta^{17}\text{O}=-30\text{‰}$  defined by spinel in A37) has implications for temperature-time estimates based on calculations [5] that we previously used to place an upper limit of 1600 K (and thus a lower limit of  $\sim 500$  years) for the integrated reaction period of diffusive exchange of CAIs. More sophisticated solid ( $\pm$ melt)-gas exchange models are being evaluated. Nevertheless, the additional WL rim and interior data strongly support the idea that CAIs were transported between at least two nebular reservoirs with distinct O-isotopic compositions, probably multiple times during this time in their history.

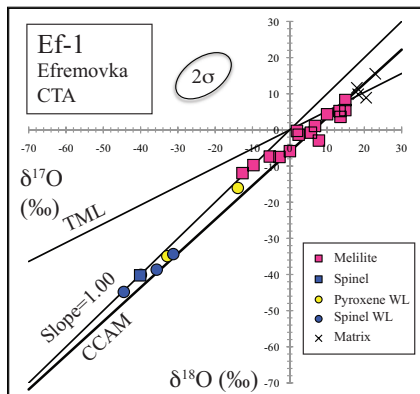


Figure 1. Oxygen three-isotope plot for Efremovka CAI Ef-1. Most data fall along the slope  $\sim 0.94$  CCAM line. Terrestrial mass fractionation (TMF) line (slope=0.52) and primordial mixing line (slope=1.00) are shown for reference. Error ellipse represents  $2\sigma$  external reproducibility.

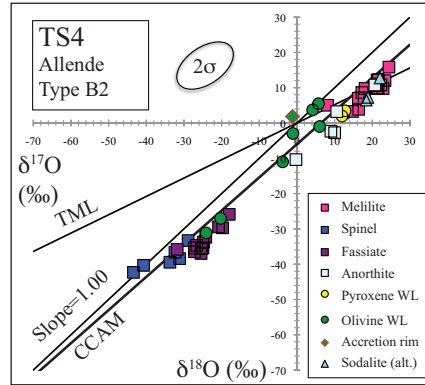


Figure 2. Oxygen three-isotope plot for Allende CAI TS4. Most data fall along the slope  $\sim 0.94$  CCAM line. Reference lines and error ellipse as in Figure 1.

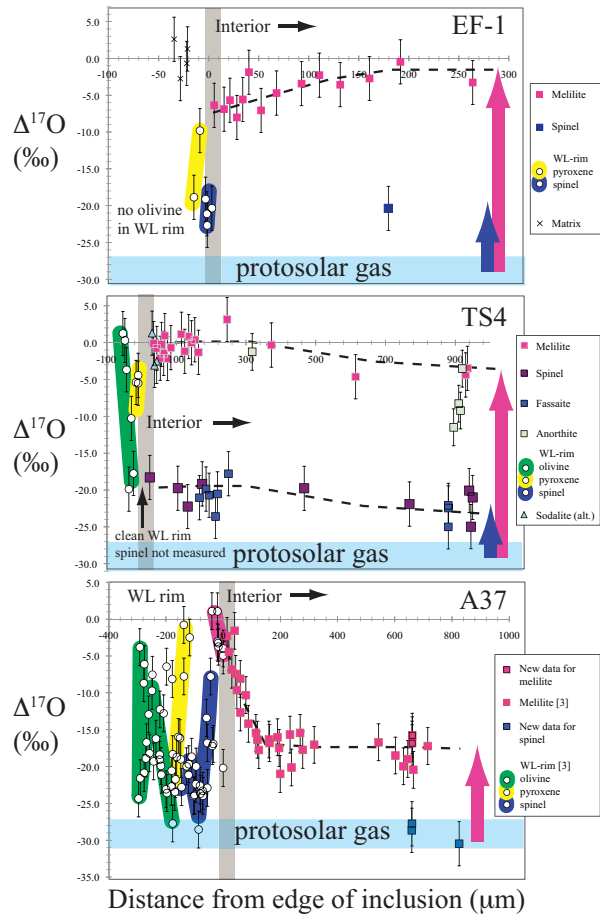


Figure 3. O-isotope zoning profiles across the WL rims and interiors of Ef-1, TS4, and A37, obtained by NanoSIMS. New data on spinel from A37 match the O-isotope composition of [4] and likely represent the primordial protosolar gas composition. Vertical arrows show the varying magnitudes of mineral-gas exchange in the studied CAIs.

References: [1] Clayton, R.N. et al. (1977), *EPSL* 34, 209-224. [2] Aleon, J. et al. (2007) *EPSL*, 263, 114-127. [3] Simon, J.I. et al. (2011) *Science*, 331, 1175-1178. [4] McKeegan, K.D. et al. (2011), *Science* 332, 1528-1532. [5] Ryerson, F.J. and K.D. McKeegan (1994) *GCA* 58, 3713-3734. [6] MacPherson, G.J., and L. Grossman (1981) *EPSL* 52, 16-24. [7] Simon, S.B. (1999) *GCA* 63, 1233-1248.